Identification of quantitative trait loci that modify the severity of hereditary spherocytosis in *wan*, a new mouse model of band-3 deficiency

Luanne L. Peters, Rebecca A. Swearingen, Sabra G. Andersen, Babette Gwynn, Amy J. Lambert, Renhua Li, Samuel E. Lux, and Gary A. Churchill

Defects in red blood cell (RBC) membrane skeleton components cause hereditary spherocytosis (HS). Clinically, HS varies significantly even among individuals with identical gene defects, illustrating the profound effects of genetic background on disease severity. We exploited a new spontaneous mouse model, *wan*, which arose on the inbred C3H/HeJ strain, to identify quantitative trait loci (QTL) that modify the HS phenotype. Homozygous *wan* mice have severe HS due to a complete deficiency of erythroid band 3. A QTL analysis of RBC count, hemoglobin, hematocrit, mean corpuscular volume (MCV), and mean corpuscular hemoglobin content (MCHC) was performed in *wan/wan* mice from an F2 intercross between C3H/HeJ[+/wan] and CAST/Ei^{+/+} F1 hybrids. Hematologic and survival data from C3H, CAST/Ei F2 *wan* homozygotes support the hypothesis that genetic modifiers significantly influence the band-3 null HS phenotype. Significant QTL were identified for the MCV trait only, suggesting that RBC membrane characteristics are a target for modifier gene action. The most significant quantitative trait locus, *Hsm1* (hereditary spherocytosis modifier 1), localizes to mouse Chromosome 12 and is dominant. The peak LOD score was obtained with a marker for *Spnb1* encoding erythroid β-spectrin, an obvious candidate gene. (Blood. 2004;103: 3233-3240)

© 2004 by The American Society of Hematology

Introduction

Hereditary spherocytosis (HS) is the most common inherited hemolytic anemia in people of Northern European descent, occurring with a frequency of approximately 1 in 2000.[1] HS is caused by defects in the red blood cell (RBC) membrane skeleton, a multiprotein structure located just beneath the lipid bilayer that imparts mechanical strength and elasticity to the RBC membrane. The major component of the membrane skeleton, spectrin, is present as tetramers of α- and β-subunits cross-linked into a 2-dimensional array by short actin filaments.[1-3] There are 2 major interactions between membrane skeleton components and integral membrane proteins that attach the spectrin array to the plasma membrane: (1) band 3–spectrin–ankyrin–protein 4.2 and (2) protein 4.1–p55–glycophorin C linkages.[4-8]

The band 3–spectrin–ankyrin–protein 4.2 interactions are critical in the pathogenesis of HS. Defects in all of these proteins cause HS in humans and in mice.[1,9,10] Recent estimates are that approximately 50% of the mutations causing HS in European populations are in ankyrin, 20% in band 3, 20% in β-spectrin, 5% in protein 4.2, and less than 5% in α-spectrin.[1] Depending on the exact genetic defect, the hematologic phenotype varies from asymptomatic to life-threatening hemolysis requiring transfusion therapy and/or splenectomy. Secondary complications of HS include jaundice, gallstones, aplastic crises, and, more rarely, extramedullary hematopoietic masses and leg ulcers.[1] In the ankyrin-deficient *nb* mouse,

progressive ataxia due to Purkinje cell degeneration occurs.[11] In other mouse models of HS, thrombosis and infarction are significant complicating factors.[12]

Many specific molecular defects that cause HS in humans have been described.[1] Notably, as in other heritable syndromes, the clinical presentation varies significantly even among individuals with identical gene defects, illustrating the profound effects of genetic background on disease severity.[10] Identifying genetic modifiers by linkage analysis in humans is often difficult, if not impossible, due to environmental influences, genetic diversity, and small population (linkage group) size. Inbred mice, however, provide powerful tools for complex trait analysis. Moreover, as concordance between quantitative trait loci (QTL) in the mouse and human has been demonstrated for several diseases, complex trait analysis in the mouse has significant biomedical relevance.[13,14]

Here, we describe a new spontaneous HS mutation in the mouse, *wan,* which arose on the C3H/HeJ (C3H) inbred strain, and identify QTL that modify the severity of the HS phenotype. Homozygous *wan* mice are severely anemic. A premature stop codon in the gene encoding erythroid band 3, *Slc4a1* (solute carrier family 4 [anion exchanger], member 1; formerly *Ae1,* anion exchanger 1), results in complete deficiency of band 3 in homozygotes. In hybrid *wan/wan* newborns derived from F2 intercrosses between C3H[wan/+] and *Mus musculus castaneus* (CAST/Ei), marked

---

phenotypic variation is observed, suggesting the presence of segregating modifier alleles. Analysis of these F2 intercross progeny failed to detect significant QTL using RBC count, hemoglobin (Hgb), hematocrit (Hct), or mean corpuscular hemoglobin content (MCHC) values as quantitative traits. However, using mean corpuscular volume (MCV), 2 significant QTL were identified, 1 on chromosome (Chr) 6 and 1 on Chr 12. The Chr 6 quantitative trait locus is very broad, spanning more than 40 cM (centimorgans), and likely represents several, closely linked QTL. The Chr 12 quantitative trait locus, designated *Hsm1* (hereditary spherocytosis modifier 1), spans 12 cM. Notably, the peak LOD score was obtained using a marker for erythroid β-spectrin *(Spnb1),* a strong candidate gene.

Materials and methods

Mice

The autosomal recessive mutation *wan* arose on the C3H/HeJ (C3H) inbred strain at The Jackson Laboratory (Bar Harbor, ME). As all C3H*wan* homozygotes die within 72 hours of birth, all studies were performed on fetuses and newborns unless otherwise noted. C3H[+/wan] mice appear overtly normal. The C3H*wan* strain was initially maintained by intercrossing progeny-tested heterozygotes and, once molecularly identified, by intercrossing typed heterozygotes (see "Genotyping of progeny"). Mice were housed in humidity- and temperature-controlled rooms with a 12-hour light cycle and free access to acidified water and chow (NIH 5K52). All protocols were approved by The Jackson Laboratory Animal Care and Use Committee. The Jackson Laboratory is fully accredited by the American Association for Accreditation of Laboratory Animal Care (AAALAC).

Complete blood counts

Whole blood ($\sim$ 30 µL) was collected from decapitated newborns in EDTA (ethylenediaminetetraacetic acid)–coated microhematocrit tubes, transferred to a clean eppendorf tube containing 1 µL 20% EDTA in murine phosphate-buffered saline (PBS; 10 mM NaCl, 155 mM KCl, 10 mM glucose, 1 mM MgCl$_2$, 2.5 mM KHPO$_4$, pH 7.4), and mixed. The additional anticoagulant is critical in preventing clot formation. Following dilution in murine PBS (1:10), complete blood counts were determined using an Advia 120 Multi-species whole blood analyzer (Bayer, Tarrytown, NY). Adult whole blood ($\sim$ 275 µL) was drawn from the retro-orbital sinus through EDTA-coated microhematocrit tubes directly into an eppendorf tube containing 30 µL 20% EDTA in murine PBS and analyzed without dilution. For fetal blood counts, whole blood ($\sim$ 5 µL) was collected and analyzed using a Coulter Counter Model ZBI (Coulter, Hialeah, FL) as previously described.[15] Reticulocytes were counted manually after staining with new methylene blue (Sigma, St Louis, MO). Of note, we previously reported an apparent failure of reticulocytosis in *wan/wan* mice.[16] However, this proved to be an artifact; new methylene blue will not stain reticulocytes in homozygous *wan/wan* blood containing excess EDTA. The protocols above preserve both RBC morphology and reticulocyte staining. Control reticulocytes (+/*wan,* +/+) do not show this EDTA sensitivity. The basis for the staining differences is unknown.

Electron microscopy

Whole blood was collected as described above and centrifuged 3 minutes at 3000*g*. The cells were washed in mouse PBS, fixed in 2% glutaraldehyde in cacodylate buffer (pH 7.4, 4°C), and examined using a Jeol JEM-100 Scanning electron microscope (Jeol USA, Peabody, MA) as previously described.[17]

Production of polyclonal band-3 antibodies

A band-3 cDNA fragment encoding amino acid 8 through amino acid 399 (encompassing nearly the entire cytoplasmic domain) was subcloned into the pGEX-2TK vector and transformed into DH5α *Escherichia coli* using standard techniques. The recombinant protein was expressed and purified as described.[18] Antibody was generated in rabbits by Strategic Biosolutions (Hercules, CA). The antibody was designated anti-cdb3.

Analysis of red cell membrane skeleton proteins

Hemoglobin-depleted RBC ghosts were prepared as described.[19] Sodium dodecyl sulfate–polyacrylamide gel electrophoresis (SDS-PAGE) was performed using 4% Steck or 5% to 10% discontinuous Laemmli gels.[20,21] Gels were stained with Coomassie blue or electrophoretically transferred to Hybond enhanced chemiluminescence (ECL) nitrocellulose membrane (Amersham International, Buckinghamshire, England) using a semidry transfer apparatus (Bio-Rad, Oxnard, CA). Immunoblots were probed with previously described rabbit polyclonal antibodies to spectrin,[22] ankyrin,[23] protein 4.1,[24] and protein 4.2[25] or antipeptide antibodies recognizing amino acids 214 to 228[26] or the C-terminal 12 amino acids of mouse band 3,[27] and with the polyclonal anti-cdb3 described above. Antibody to human βIΣ2 spectrin[28] was kindly provided by Dr Jon S. Morrow (Yale University, New Haven, CT). Bound antibody was detected with goat antirabbit horseradish peroxidase (HRP)–conjugated immunoglobulin G (Bio-Rad) and visualized using ECL detection reagents (Amersham International).

Northern blotting

Total RNA was isolated from newborn reticulocytes as described.[29] Northern blotting was performed using standard techniques. A 3.0-kb mouse band-3 cDNA probe encompassing the entire open reading frame (GenBank accession no. X02677) was used as the hybridization probe.

Identification of the *wan* gene defect

Genomic DNA was prepared from tail samples (Gentra Systems, Minneapolis, MN) and used as a template for the polymerase chain reaction (PCR). Band 3–specific primers approximately 20 base pairs in length with approximately 50% GC composition were designed flanking each exon (primer sequences available upon request). The PCR was carried out in an MJ Research PTC-200 Thermocycler (MJ Research, Watertown, MA) for 40 cycles (94°C, 15 seconds; 55°C, 30 seconds; 72°C, 1 minute) with a 15-minute incubation at 72°C following the last cycle. The products were subcloned into the pCR 2.1 vector (Invitrogen, Carlsbad, CA) and sequenced using the automated dye termination technique (ABI Systems, Foster City, CA).

Genotyping of progeny

The *wan* mutation generates an additional *Bfa*I site, allowing genotyping of progeny (see "Results"). Genomic DNA was prepared and amplified as described above. The oligonucleotides (5′ → 3′) GGCCTTTTCTAAGCCTAGCT and CCAGAAAGCCACCTATGCAG were used as forward and reverse primers, respectively. The PCR products were digested overnight and resolved on a 2% NuSieve gel (BioWhittaker Molecular Applications, Rockland, ME).

β-spectrin sequencing

Genomic DNA was obtained from The Jackson Laboratory DNA Resource (http://www.jax.org/dnares/index.html). The PCR was carried out as above using oligonucleotides flanking each exon of the mouse β-spectrin gene (sequences available upon request). The products were sequenced using the automated dye termination technique (ABI Systems).

QTL analyses

To identify QTL influencing the *wan* phenotype, an F2 intercross between C3H*wan/+* and wild-type *Mus musculus castaneus* (CAST/Ei) mice was established. Complete blood counts and genotyping of F2 progeny at birth were performed as described above. Simple sequence length polymorphic (sslp) markers spaced at 10- to 30-cM intervals throughout the genome were typed by the PCR using multiplexed fluorescent markers and ABI 3700 instrumentation. After identification of QTL, additional markers spaced at 2- to
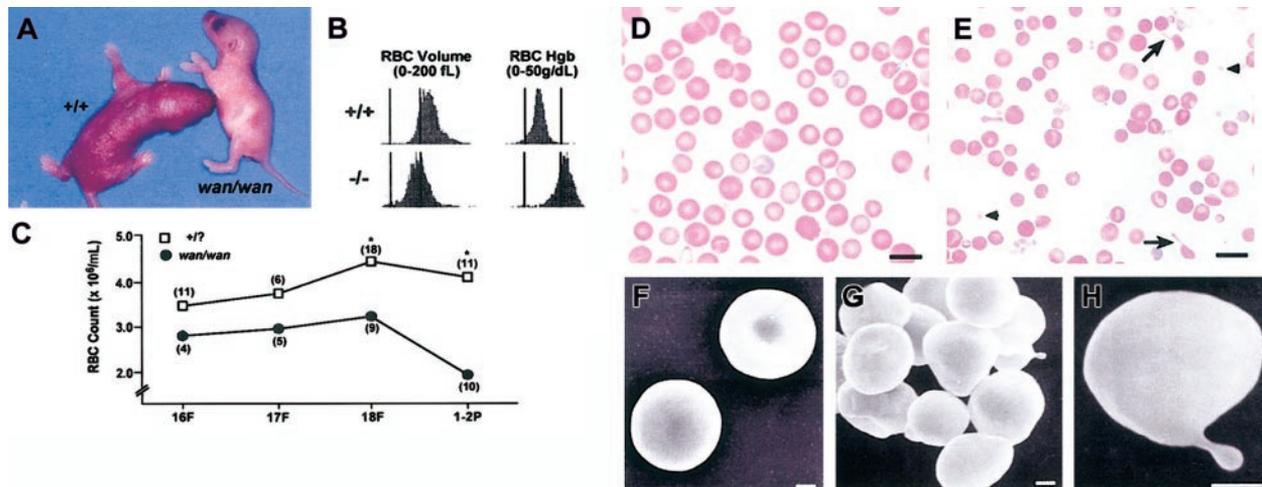
Figure 1. Hematologic status of C3H/HeJ_wan_ **homozygotes.** (A) A C3H/HeJ_wan/wan_ newborn with a wild-type (+/+) littermate. Note the extreme pallor of the _wan_ homozygote. (B) RBC volume and hemoglobin concentration histograms of whole blood from normal (+/+) and _wan/wan_ (−/−) newborn mice. Significant populations of small (left panels) and dehydrated (right panels) RBCs are present in mutant blood compared with controls. (C) RBC counts are decreased in _wan/wan_ fetuses compared with normal littermates. The differences are significant (*$P < .001$) by fetal day 18 and at birth. (D-E) Wright-stained peripheral blood smear from a newborn C3H$^{+/+}$ mouse (D) and a mutant C3H$^{wan/wan}$ mouse (E). Many RBC fragments (arrowheads) and membrane projections (arrows) are evident in mutant blood smears. Bar = 10 μM. (F-H) Scanning electron photomicrographs of normal (F) and mutant (G-H) RBCs. Mutant RBCs are predominantly spherocytic (G) with frequent membrane projections (H). Bar = 1 μM.

9-cM intervals on Chr 12 were added. Primers were purchased from Research Genetics (MapPairs, Huntsville, AL).

Genome-wide scans were performed using RBC count, Hgb, Hct, MCV, and MCHC as quantitative traits. Results were analyzed by forward stepwise multiple regression analysis using sex and body weight as additive covariates.[30] Genome-wide scans were performed using Pseudomarker software (source codes available at http://www.jax.org/staff/churchill/labsite/software/pseudomarker/index.html).[31] Significance thresholds were determined by permutation analysis in which the regression analysis is performed on randomized genetic marker and phenotypic data.[32] The significant LOD score is that giving a P value of .05, whereas suggestive is a P value of .10. Confidence intervals were determined by computing the region of the posterior density curve containing 95% of the total area as described by Sen and Churchill.[31] A simultaneous search for pairs among QTL was performed as described.[13,31] Pairwise genome scans can detect QTL that affect a phenotype by interacting with another quantitative trait locus (including those instances where neither quantitative trait locus alone reaches the significance threshold).

Results

Wan mice have severe HS

Homozygous _wan_ mice are recognizable at birth by their extreme pallor (Figure 1A). Newborns are severely anemic (Table 1) and smaller than normal littermates. The RBC count, Hgb, Hct, MCV, and mean corpuscular hemoglobin (MCH) are significantly decreased compared with wild-type (+/+) littermates (Table 1). The MCHC is significantly increased. RBC volume and RBC hemoglobin concentration histograms reveal a significant population of

microcytic and dehydrated cells (Figure 1B). Reticulocytes are increased nearly 2-fold ($56.6 \pm 8.0\%$ [X ± SD] [n = 5] in _wan_ homozygotes vs $30.6 \pm 9.7\%$ [n = 8] in +/+ littermates; $P < .001$). Male and female _wan/wan_ mice do not differ significantly from each other in any of these hematologic parameters. Values for heterozygotes (+/_wan_) do not differ significantly compared with wild type except for the MCV, which is significantly lower (85.0 ± 4.0, n = 19, $P < .001$; see +/+ data in Table 1).

Crosses between heterozygotes yield the expected Mendelian ratio of anemic offspring, indicating no significant fetal loss. However, anemia is present in utero. Decreased RBC counts are apparent by fetal day 16 (Figure 1C). By fetal day 18, RBC counts are significantly lower than in normal littermates. RBC counts decrease temporarily in normal neonates.[15] In _wan/wan_ mice, this drop is precipitous; newborn counts decrease to 50% of the levels seen on fetal day 18. In comparison, in normal neonates, the RBC count decreases much less, to 90% of its value on fetal day 18.

Examination of neonatal _wan_ peripheral blood smears reveals marked anisocytosis and spherocytosis (Figure 1D-E). By scanning electron microscopy, _wan_ RBCs are severely spherocytic and membrane protrusions are evident (Figure 1F-H). The hematologic data and RBC morphology are consistent with the phenotype of severe HS.

Band 3 and protein 4.2 are absent in _wan_ red cell membrane skeletons

Analysis of RBC ghost membranes by SDS-PAGE and Western blotting reveals normal or near normal levels of spectrin and

Table 1. Hematologic parameters in newborn mice

Genotype	n	RBC count, × 10^{12}/L	Hgb, g/L	Hct	MCV, fL	MCH, pg	MCHC, g/dL
C3H/HeJ$^{+/+}$	9	3.6 ± 0.5 (2.9-4.4)	111 ± 15 (90-140)	0.332 ± 0.035 (0.27-0.38)	91.5 ± 2.9 (87.1-96.0)	30.1 ± 2.4 (27.0-33.6)	32.9 ± 2.1 (29.4-36.3)
C3H/HeJ$^{wan/wan}$	18	$1.8 \pm 0.5*$ (1.0-2.6)	$48 \pm 15*$ (20-70)	$0.133 \pm 0.042*$ (0.06-0.19)	$71.9 \pm 6.0*$ (59.6-83.7)	$25.8 \pm 3.4†$ (18.2-30.5)	$36.4 \pm 3.5‡$ (28.5-41.7)

Complete blood counts were obtained using an Advia 120 Multi-species hematology analyzer. All values are ± SD, and values in parentheses represent ranges.

*$P < .001$.
†$P < .01$.
‡$P < .05$ C3H/HeJ$^{wan/wan}$ versus C3H/HeJ$^{+/+}$ (2-tailed Student t-test).
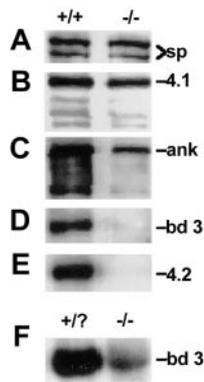
Figure 2. Membrane skeleton proteins in *wan* homozygotes. (A-E) Western blots showing levels of spectrin (sp, A), protein 4.1 (4.1, B), ankyrin (ank, C), band 3 (bd 3, D), and protein 4.2 (4.2, E) in normal (+/+) and *wan/wan* (−/−) RBC ghosts. Note the absence of band 3 and protein 4.2 and the decrement of ankyrin in mutant RBCs. In panel D, a peptide antibody raised to amino acids 214 to 228 of the cytoplasmic domain of band 3 was used. The same result was obtained using a pan-cytoplasmic domain band-3 antibody as well as a peptide antibody recognizing the C-terminal 12 amino acids of the membrane spanning domain, confirming that *wan* homozygotes are band-3 null. (F) Northern blot showing the severe decrement in band-3 mRNA in *wan* homozygotes. Each lane contains 2 μg total RNA purified from 2 pooled mutant (−/−) and 4 phenotypically normal (+/?) newborn peripheral blood samples whose genotypes were subsequently confirmed by PCR (see "Materials and methods").

protein 4.1 in *wan* homozygotes (Figure 2A-B). Ankyrin is substantially decreased, whereas band 3 and protein 4.2 are absent (Figure 2C-E). As remarkably similar phenotypes were observed in 2 previously described targeted band-3 null mouse models,[33,34] we intercrossed +/*wan* and targeted band-3 heterozygotes generated in our laboratory.[34] The crosses yielded the expected Mendelian frequency of anemic offspring. Together, the data indicate that the *wan* gene defect lies within the erythroid band-3 gene. Consistent with these findings, *wan* reticulocyte band-3 mRNA levels were decreased to approximately 10% of normal (Figure 2F).

Sequencing reveals a premature stop codon in the *wan Ae1* gene

Band-3 exons from homozygous *wan* mice and C3H^{+/+} controls were amplified from genomic DNA, subcloned, and sequenced. A single base transition (C>T) at nucleotide 3998 (GenBank accession no. J02756) in *wan* was identified. The change introduces a premature stop codon (TAG) in place of glutamine (Gln) (CAG) at amino acid 85, which lies within the cytoplasmic domain of band 3, close to the N-terminus (Figure 3A). No other nucleotide changes in band-3 exons or splice junctions were found in C3H[wan] versus C3H^{+/+} genomic DNA. The transition at nucleotide 3998 generates a *Bfa*I restriction site, which was exploited for genotyping purposes (Figure 3B).

Evidence for segregating modifier genes in band-3 null mice

Band-3 null mice maintained on different genetic backgrounds show striking phenotypic differences. All homozygous C3H[wan] inbred mice die within 72 hours of birth. In contrast, 75% of the knock-out band-3 null mice (B6,129 Bd3^{−/−}) maintained on a hybrid C57BL/6J (B6) and 129/Sv (129) genetic background survive beyond 72 hours, with 15% surviving to adulthood (Figure 4A).[34] Notably, more than 99% of B6 congenic Bd3^{−/−} mice (n = 15) die in utero. This is remarkable given the molecular similarities of the 2 models. No band-3 protein is produced in red cells of either the knock-out or the spontaneous model, and the kidney transcript, which uses a separate start codon upstream of the *wan* premature stop codon,[35] is disrupted in both. Both mutations result in severe anemia. Surprisingly, B6,129 Bd3^{−/−} newborns

appear to be more severely anemic than *wan* homozygotes despite their overall improved survival. RBC counts, Hgb, and Hct values are significantly lower and the reticulocyte percentage is significantly higher compared with *wan/wan* newborns (Figure 4B).

We also noted that some C3H, CAST/Ei F2 [wan/wan] newborns lacked significant pallor and could be identified with confidence only by genotyping. Moreover, some survived well beyond the 72-hour maximum observed for inbred C3H *wan* mice (up to 5 months). To examine this more closely, we allowed a subset of F1 mating pairs to give birth and rear their young undisturbed. Of 188 weaned (3-4 weeks of age) offspring, 10 *wan/wan* mice were identified, well below the number of *wan* homozygotes expected based on Mendelian inheritance of a recessive allele (25%). Assuming that homozygosity at the *wan* locus is the only genetically determined cause of mortality in all offspring prior to weaning, we can infer the number of *wan/wan* animals that died prior to weaning. Using the number of live +/+ (65) and +/*wan* (113) animals and the expected 25%:50%:25% ratio of +/+-to-+/*wan*-to-*wan/wan* F2 offspring, we predict that a total of 60 *wan/wan* mice were born. Hence, as in the band-3 knock-out model, a mixed genetic background markedly improves survivability in *wan* homozygotes, from 0% on C3H to 17%. Taken together, the observations of the various band-3 null strains indicate that genetic background profoundly influences the band-3 null HS phenotype in terms of survival and basic hematologic parameters.

Identification of genetic loci that modify the band-3 null phenotype

Complete blood counts were performed in a total of 670 C3H, CAST/Ei F2 *wan/wan* mice. Of these, 183 (27%) were homozygous *wan* with the expected ratio of males and females (53% female). As in the inbred C3H[wan] strain, the RBC count, Hgb, Hct, MCV, and MCH are significantly decreased, and the MCHC is significantly increased, in homozygous C3H, CAST F2 *wan* mice compared with F2 wild-type mice (Table 2). Notably, F2 *wan/wan* newborns show an extremely broad range of values for all parameters, and these values significantly overlap the normal ranges seen in F2 wild-type mice (Table 2). The F2 hematologic data further confirm the profound effect of genetic background,
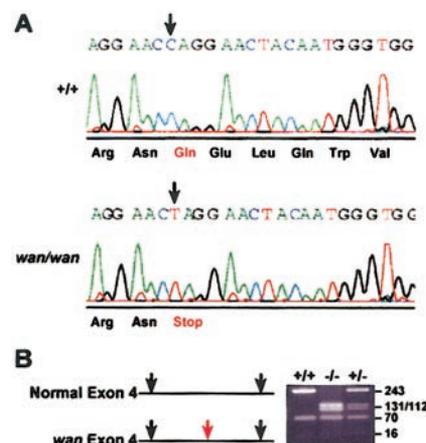

Figure 3. Premature stop codon in the *wan* band-3 gene. (A) Chromatogram showing the sequence of *Slc4a1* encoding erythroid band-3 in control (+/+) and *wan/wan* genomic DNA. In *wan* homozygotes, a C>T transition (arrows) results in a premature stop codon at amino acid 85 within the cytoplasmic domain of band 3. (B) *Bfa*I restriction digest of PCR-amplified products from control (+/+), homozygous (−/−), and heterozygous (+/−) mice resolved on a 2% NuSieve gel. The transition in the band-3 gene in *wan* creates an additional *Bfa*I site (red arrow) that was exploited to genotype mice.

Figure 4. Phenotypic differences between band-3 null strains maintained on different genetic backgrounds. (A) Of inbred band-3 null C3H/HeJ*wan/wan* mice, 100% die within 72 hours of birth (○), whereas a targeted strain of band-3 null mice maintained on a hybrid (B6, 129) genetic background show significantly less early mortality, with approximately 15% surviving to adulthood (●). (B) Hematologic analysis of newborn mice obtained using an Advia Multi-species whole-blood analyzer reveals severe anemia in both band-3 null strains, although significant differences are seen. *$P < .01$; **$P < .001$. Error bars indicate standard error.
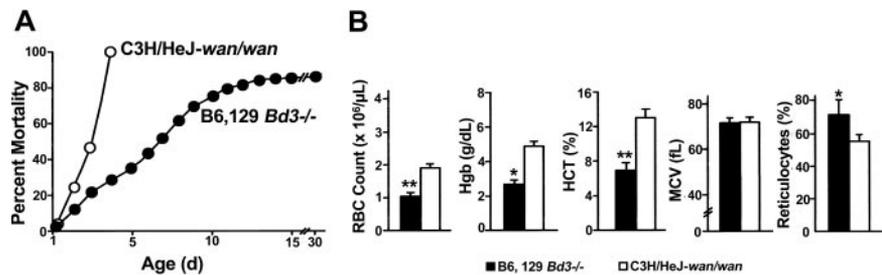
indicating that the CAST/Ei parent is contributing an allele(s) that significantly influences the band-3 null HS phenotype.

To identify modifiers of the *wan* phenotype, we performed genome-wide scans of F2 *wan/wan* mice using RBC count, Hgb, Hct, and MCV as quantitative traits with sex and weight as additive covariates. A total of 96 markers was genotyped. In an initial scan of 94 F2 animals, a single suggestive quantitative trait locus on Chr 12 was identified using MCV as trait (not shown). No other suggestive or significant QTL were identified using RBC count, Hgb, or Hct as traits. These data suggested that the QTL could influence the HS phenotype by modifying RBC membrane characteristics such as the extent of membrane vesiculation and/or the rate of cation and water loss, both of which would be expected to alter the MCV value. The marker *D12Mit156*, located 32 cM distal to the centromere, gave the peak LOD score. Notably, the gene encoding erythroid β-spectrin, *Spnb1*, maps to this region of mouse Chr 12.[35] Spectrin could influence membrane characteristics in a number of ways and is an obvious candidate gene. Therefore, we generated additional F2 animals and added several polymorphic markers mapping to this region of Chr 12, including β-spectrin (see "Materials and methods"), and repeated the analyses using the same traits as above plus the MCHC value. Analysis of 183 F2 animals identified 2 significant QTL using MCV as trait—the previously suspected Chr 12 quantitative trait locus and a second quantitative trait locus on Chr 6 (Figure 5A). Again, no significant QTL were identified using the RBC count, Hgb, or Hct as trait in this analysis. No sex differences were seen. A simultaneous search for pairs to detect interacting QTL was negative. The maximum LOD score for the Chr 12 MCV quantitative trait locus (3.7) was obtained with the β-spectrin marker and exceeds the minimum LOD score for significance (2.2) (Figure 5A-B). The 95% confidence limits for the QTL span from 28 to 40 cM on Chr 12 (Figure 5B). As this quantitative trait locus is a modifier of hereditary spherocytosis, we have designated the locus *Hsm1* (hereditary spherocytosis modifier 1). The allele effects of *Hsm1* on red cell volume are shown in Figure 5C; the presence of 1 or 2 CAST alleles at the β-spectrin locus significantly lowers the MCV, suggesting *Hsm1* is dominant. *Hsm1* accounts for 9% of the total variance of the trait.

The second MCV quantitative trait locus, located on Chr 6, is extremely broad, spanning approximately 40 cM (Figure 5D). This quantitative trait locus likely represents several closely linked loci, as revealed by the distinct "shoulders" seen in the genome scan

(Figure 5D), that together account for 7% of the variance of the trait. No significant QTL were identified using the MCHC as the quantitative trait. However, suggestive QTL were identified on Chr 7 and 19 (Figure 5A). Further analyses using additional markers to saturate the relevant chromosomal intervals and increased numbers of F2 mice will be required to determine the exact number of QTL on Chr 6 and to determine if the MCHC QTL reach statistical significance.

Red cell morphology is markedly pleiotropic in C3H, CAST F2 mice

The data suggest that changes in RBC membrane characteristics, which are reflected in the MCV value, may modify the HS phenotype. If membrane characteristics are indeed influenced by a segregating modifier in our F2 intercross, one would expect to see widely varying RBC morphology among the F2 *wan* homozygotes, as is the case with other hematologic parameters (Table 2). Peripheral blood smears confirm this expectation. A subset of F2 *wan/wan* mice shows extremely aberrant red cell morphology (Figure 6A) similar to that seen in inbred C3H*wan* homozygotes (Figure 1E), that is, striking anisocytosis with extreme microcytosis. Indeed, many RBC fragments smaller than platelets and frequent cells with tubular membrane extensions are present. Other F2 *wan* homozygotes, however, show markedly improved overall red cell morphology (Figure 6B). It should be emphasized that the smears presented in Figure 6 represent the extremes of RBC morphologies seen in the F2 population. The majority of slides examined revealed morphologic characteristics intermediate to these 2 extremes.

Spnb1 encoding β-spectrin is a candidate gene for *Hsm1*

Spnb1 encoding erythroid β-spectrin is located within the QTL interval at 33 cM.[36] No other RBC membrane proteins or obvious candidate genes map within the *Hsm1* critical interval on mouse Chr 12. We sequenced the entire *Spnb1* cDNA in the parental strains, C3H and CAST/Ei, as well as in 2 additional inbred strains, B6 and 129. The amino acid sequence was identical in C3H, B6, and 129. There were 3 amino acid differences found in the CAST/Ei sequence: M1003V (C3H → CAST), corresponding to amino acid 19 of repeat 7; M1238K, amino acid 80 of repeat 9; and R1571C, amino acid 103 of repeat 12 (numbering according to Genbank sequence NM013675). None of these changes suggests an

Table 2. Hematologic parameters in newborn C3H, CAST F2 mice

Genotype	n	RBC count, × 10^{12}/L	Hgb, g/L	Hct	MCV, fL	MCH, pg	MCHC, g/dL
C3H,CAST$^{+/+}$	148	3.7 ± 0.6 (2.2-5.4)	111 ± 20 (64-160)	0.347 ± 0.054 (0.2-0.52)	95.1 ± 5.9 (80.7-111.2)	30.2 ± 2.6 (23.7-38.4)	31.8 ± 2.6 (25.0-37.5)
C3H,CAST-*wan/wan*	183	2.2 ± 0.7* (0.7-5.2)	62 ± 20* (16-130)	0.174 ± 0.058* (0.048-0.4)	79.9 ± 6.9* (62.3-95.3)	28.2 ± 3.6* (17.8-36.4)	35.3 ± 3.4* (25.0-46.2)

Complete blood counts were obtained using an Advia 120 Multi-species hematology analyzer. All values are ± SD, and values in parentheses represent ranges. *$P < .001$ (2-tailed Student *t* test).
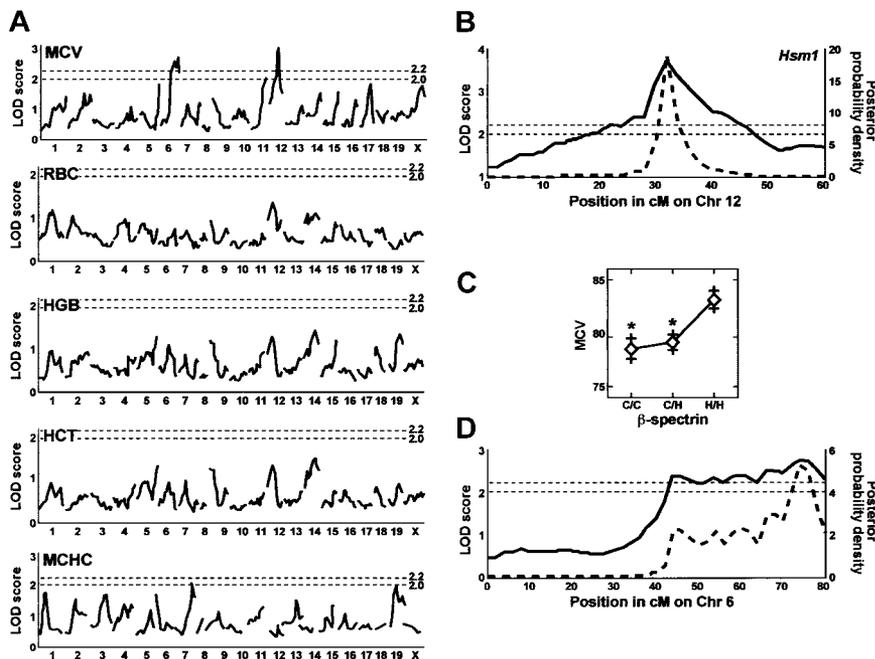
Figure 5. QTL analysis of F2 *wan* homozygotes. (A) Genome-wide scan of MCV, RBC count, Hgb, Hct, and MCHC. Significant QTL (minimum LOD score of 2.2, indicated by the top dashed line) were detected on Chr 6 and Chr 12 using MCV as the quantitative trait. No suggestive (LOD score of 2.0, indicated by the bottom dashed line) or significant LOD scores were obtained using RBC count, Hgb, or Hct as traits, but 2 suggestive QTL are seen for the MCHC. (B) Interval map of the Chr 12 MCV quantitative trait locus (solid line) showing the position (cM) of the markers. This quantitative trait locus was designated *Hsm1*. The peak LOD score for *Hsm1* was obtained using a marker for the erythroid β-spectrin gene (*Spnb1*). The posterior probability density curve corresponding to the 95% confidence interval (bold dashed line) was computed by the method of Sen and Churchill.[31] This analysis shows that the 95% confidence interval for *Hsm1* is between 28 and 40 cM. (C) Allele effects of *Hsm1* using the peak LOD score marker (*Spnb1*, β-spectrin) indicates that it acts as a dominant and lowers the MCV. C indicates CAST/Ei *Spnb1* allele; H, C3H *Spnb1* allele. *P < .01. Error bars indicate standard error. (D) Interval map of the Chr 6 MCV quantitative trait locus reveals multiple shoulder peaks, indicating that several QTL are likely present in the interval. The 95% confidence interval is between 40 and 80 cM. The peak LOD score was obtained with *D6Mit15*.

obvious mechanism whereby the CAST/Ei allele might influence membrane characteristics. In addition, no differences in β-spectrin protein levels between the parental strains, C3H and CAST/Ei, are detectable by Western blotting of mature RBC membrane ghosts, nor are there any differences in the amount of spectrin retained following low salt extraction (data not shown). Reverse transcriptase–PCR of fetal liver RNA and Western blotting of RBC ghosts failed to detect the presence of the pleckstrin homology (PH) domain in either strain (not shown), suggesting that strain differences in the regulation of the alternatively spliced "muscle" spectrin isoform (β1Σ2)[28] are not present. Nevertheless, β-spectrin remains a candidate for *Hsm1* for reasons discussed below.

Discussion

To dissect modifier genes critical to the pathogenesis of band 3–deficient HS, we mapped QTL influencing the *wan* phenotype. No significant QTL were detected when RBC count, Hgb, Hct, or MCHC values were used as quantitative traits, suggesting that these RBC characteristics are not significant targets for modifying genes in our cross. However, 2 significant QTL were identified using MCV as trait. It is noteworthy that the MCV is a directly measured trait on the Advia 120 hematology analyzer. Moreover, as the F2 *wan* homozygotes had similarly elevated reticulocyte counts, varying degrees of reticulocytosis are unlikely to have significantly influenced the MCV in the F2 population.

The first MCV quantitative trait locus spans a 40-cM interval on the distal half of Chr 6 and probably represents several QTL. The only RBC membrane skeleton gene on mouse Chr 6 is *Add2* encoding β-addu-cin.[36] *Add2* is located proximal to the QTL interval at 35.5 cM, making it an unlikely candidate gene. The size of the interval precludes meaningful analysis of other potential candidate genes at this time. To identify all the QTL within the interval and candidate genes for each will require additional F2 animals and sufficient markers to saturate the relevant portion of Chr 6.

The second significant QTL interval, which we have designated *Hsm1,* is a single peak that spans a 12-cM interval on mouse Chr 12. Analysis of allele effects indicates that *Hsm1* acts in a dominant fashion. Interestingly, both the Chr 6 modifying gene(s) and *Hsm1* were identified using the MCV as the quantitative traiting suggest that RBC membrane characteristics are a target for modifier gene action in band-3 null HS. Moreover, heterozygous C3H[+/wan] mice do not differ from wild-type C3H^{+/+} controls in any hematologic
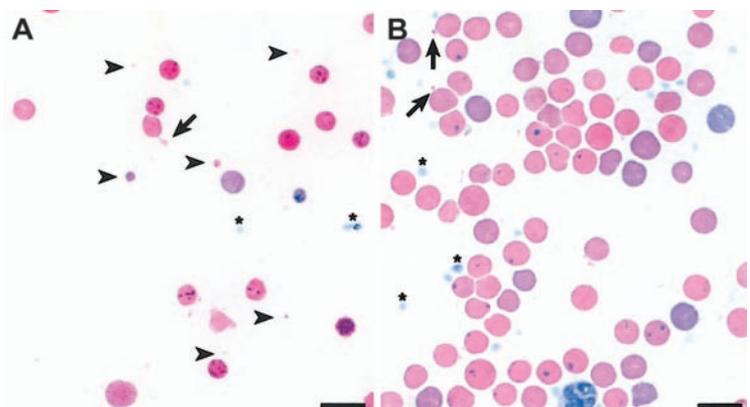

Figure 6. Pleiotropic RBC morphologies in F2 *wan* homozygotes. (A) Wright-stained peripheral blood smear showing extreme microspherocytosis and tubular membrane extensions (arrow). Note that some microcytes (arrowheads) are smaller than platelets (asterisks). (B) Peripheral blood smear showing significantly improved overall RBC morphology. Evidence of some membrane loss, however, persists (arrows). Bar = 10 μM.

parameter *except* the MCV, suggesting that the MCV value is the most sensitive surrogate for band-3 deficiency.

The peak LOD score on Chr 12 is obtained with the *Spnb1* gene encoding erythroid β-spectrin. Of the 3 β-spectrin polymorphisms identified between the C3H and CAST/Ei inbred strains, none occurs in domains known to influence the binding of spectrin to the membrane, for example, the ankyrin binding domain bridging spectrin repeats 14 and 15 and the membrane association domain 1 (MAD1) in repeat 1, which mediates ankyrin- and protein 4.1–independent spectrin binding to the membrane.[37,38] In addition, we were unable to detect any gross differences between the parental strains in RBC β-spectrin protein levels or differences in the amount of spectrin remaining in resealed RBC ghosts following low salt extraction by Western blotting. Such preliminary data seem to argue against β-spectrin as a legitimate candidate for *Hsm1*. However, homozygosity at the *Hsm1* locus per se is not associated with hemolysis in either C3H or CAST/Ei wild-type mice. Hence, *Hsm1* polymorphisms are likely to be significant *only in the presence of the wan defect;* differences in the parental strains would therefore not be expected. Such epistatic gene interactions between mutant genes and QTL have been described previously in several other mouse mutations.[39,40] Alternatively, the application of more sensitive testing methods may detect subtle differences in C3H versus CAST spectrin function. It is noteworthy that many spectrin repeats with no known function are highly conserved across species, suggesting that spectrin likely participates in other, as yet undefined, processes within the red cell.[1]

That 17% of C3H, CAST/Ei F2 *wan/wan* mice survived to adulthood is telling evidence of the strong influence of genetic modifiers. Clearly, however, genetic factors other than *Hsm1* are also influencing the band-3 null phenotype as judged by 2 criteria. First, we identified additional QTL on Chr 6. Second, the β-spectrin sequence in B6 and 129 mice is identical to that of C3H. Despite this, B6, 129 hybrid and congenic B6 (n = 15) band-3 knock-out mice have significantly different survival rates compared with each other and with C3H*wan* homozygotes.

By what mechanism(s) might a genetic modifier of band 3–deficient HS influence RBC membrane characteristics? Band 3 is hypothesized to stabilize the lipid bilayer in 2 ways, skeleton anchoring and lipid anchoring.[1] According to the skeleton anchoring hypothesis, the bilayer is stabilized by direct interactions with the underlying spectrin array. As a major attachment site for the spectrin array, band 3 plays a pivotal role in anchoring the skeleton in place and ensuring a normal membrane spectrin content. In the "lipid anchoring" hypothesis, the bilayer is stabilized by interactions between lipids and integral membrane proteins within the horizontal plane of the bilayer. The approximately 10^6 copies of band 3 per RBC, each consisting of a transmembrane domain that traverses the lipid bilayer 14 times, are predicted to contribute significantly to lipid anchoring.[41] The primary evidence for lipid anchoring comes from the observation that band-3 deficiency in humans and mice is associated with membrane loss despite an intact membrane skeleton with normal spectrin content.[1,34] Of note, these 2 mechanisms are not mutually exclusive and likely not all inclusive. A recent study suggests that both are important and can compensate for each other to reduce the impact of membrane skeleton defects while pointing out that many observations cannot be accounted for by either mechanism, alone or in combination, indicating that other factors must contribute to the overall integrity and stability of the membrane.[42]

Thus, polymorphisms in β-spectrin could influence membrane stability in a number of ways. In both mice and humans, defects in spectrin are associated with membrane instability as well as altered cation transporter activities.[1,9,43,44] Either mechanism could potentially alter the MCV. Other mechanisms are also possible, however. For example, spectrin is known to interact with phosphatidylserine (PS) at multiple sites, and this interaction is mediated by the β-subunit.[45,46] Hence, β-spectrin polymorphisms could enhance spectrin-PS interactions. Alternatively, polymorphic β-spectrin alleles could bind other, currently unknown, integral membrane proteins with differing affinities. Finally, spectrin self-association, ankyrin binding, and band-3 binding have been shown to be coupled in a positively cooperative manner.[47] Loss of band 3, therefore, is expected to weaken spectrin self-association. β-spectrin polymorphisms may influence this positive cooperativity in such a way that it is less sensitive to the loss of band 3.

Hsm1 acts in a dominant manner to decrease the MCV. It seems intuitive that a beneficial quantitative trait locus would increase the MCV toward a normal level. Hence, a legitimate question is whether the *Hsm1-wan* interaction is detrimental rather than beneficial. The present data do not allow for a definitive assignment. The presence of CAST/Ei alleles is clearly associated with improved survival, RBC morphology, and hematologic status in a subset of the F2 hybrid animals. As several QTL are segregating, it is likely that a combination of modifier alleles, which individually may act to exacerbate or ameliorate the *wan* phenotype, acts in concert to produce the phenotypic variation seen in the hybrid *wan* homozygotes.

The definitive identification of *Hsm1* and its function will require construction of reciprocal recombinant congenic strains and bioinformatic approaches to further decrease the QTL interval and, ultimately, a transgenic or knock-out/knock-in approach to verify the most likely candidate gene.[48] To define the precise mechanism of *Hsm1* function, studies such as ektacytometry, which provide independent measurements of surface area and volume, and membrane lipid analysis will be required. Comparing congenic/targeted strains with the original C3H-*wan* mice in these and other parameters will clarify the mechanism of *Hsm1* modification of HS severity and shed light on basic mechanisms of membrane stabilization.

Classical twin studies have shown that there is a substantial genetic component underlying Hgb, RBC, white blood cell (WBC), and platelet numbers in humans.[49] The normal phenotypic variation seen among the inbred strains for these and other hematologic values, including the MCV, is clear evidence for genetic determinants in mice as well,[50] and we have identified QTL for MCV in crosses between normal inbred strains (L.L.P and G.A.C., unpublished data, November 2003). Moreover, variation in hematologic parameters is known to affect disease severity. For example, the baseline WBC count directly correlates with severity of disease symptoms in sickle cell patients.[51,52] It is clear, therefore, that basic hematologic parameters are strongly influenced by genetic factors, which in turn affect disease outcome. The determination of the genes underlying *Hsm1* and the Chr 6 quantitative trait locus, and the identification of other QTL as well, will ultimately identify genetic interactions critical to RBC stability and/or survival and the pathogenesis of HS.

Acknowledgments

References

1. Walensky LD, Narla M, Lux SE. Disorders of the red cell membrane. In: Handin RI, Lux SE, Stossel TP, eds. Blood: Principles and Practice of Hematology. 2nd ed. Philadelphia, PA: Lippincott, Williams, & Wilkins; 2003:1709-1858.

2. Gilligan DM, Bennett V. The junctional complex of the membrane skeleton. Semin Hematol. 1993;30:74-83.

3. Bennett V, Gilligan DM. The spectrin-based membrane skeleton and micron-scale organization of the plasma membrane. Ann Rev Cell Biol. 1993;9:27-66.

4. Davis LH, Bennett V. Mapping the binding sites of human erythrocyte ankyrin for the anion exchanger and spectrin. J Biol Chem. 1990;265:10589-10596.

5. Rybicki AC, Schwartz RS, Hustedt EJ, Cobb CE. Increased rotational mobility and extractability of band 3 from protein 4.2-deficient erythrocyte membranes: evidence of a role for protein 4.2 in strengthening the band 3-cytoskeleton linkage. Blood. 1996;88:2745-2753.

6. Reid ME, Chasis JA, Mohandas N. Identification of a functional role for human erythrocyte sialoglycoproteins β and γ. Blood. 1987;69:1068-1072.

7. Workman RF, Low PS. Biochemical analysis of potential sites for protein 4.1-mediated anchoring of the spectrin-actin skeleton to the erythrocyte membrane. J Biol Chem. 1998;273:6171-6176.

8. Marfatia SM, Lue RA, Branton D, Chishti AH. Identification of the protein 4.1 binding interface on glycophorin C and p55, a homologue of the *drosophila discs-large* tumor suppressor protein. J Biol Chem. 1995;270:715-719.

9. Peters LL, Barker JE. Spontaneous and targeted mutations in erythrocyte membrane skeleton genes: mouse models of hereditary spherocytosis. In: Zon LI, ed. Hematopoiesis: A Developmental Approach. New York, NY: Oxford University Press; 2001:582-608.

10. Tse WT, Lux SE. Red blood cell membrane disorders. Brit J Haematol. 1999;104:2-13.

11. Peters LL, Birkenmeier CS, Bronson RT, et al. Purkinje cell degeneration associated with erythroid ankyrin deficiency in *nb/nb* mice. J Cell Biol. 1991;144:1233-1241.

12. Barker JE, Wandersee NJ. Thrombosis in heritable hemolytic disorders. Curr Opin Hematol. 1999;6:71-75.

13. Sugiyama F, Churchill GA, Higgins DC, et al. Concordance of murine quantitative trait loci for salt-induced hypertension with rat and human loci. Genomics. 2001;71:70-77.

14. Paigen K. Understanding the human condition: experimental strategies in mammalian genetics. ILAR J. 2002;43:123-135.

15. Peters LL, Birkenmeier CS, Barker JE. Fetal compensation of hemolytic anemia in mice homozygous for the normoblastosis, *nb*, mutation. Blood. 1992;80:2122-2127.

16. Peters LL, Swearingen RA, Gwynn B, et al. Failure of effective reticulocytosis in a new spontaneous band 3 deficient mouse strain (C3H/HeJ-*wan*) and in a subset of targeted band 3 null mice (B6,129 AE1$^{-/-}$) suggests the presence of genetic modifiers of band 3 function in red blood cells [abstract]. Blood. 1998;92:301a.

17. Peters LL, Jindel HK, Gwynn B, et al. Mild spherocytosis and altered red cell ion transport in mice with a targeted deletion of the erythrocyte protein 4.2 gene (*Epb4.2*). J Clin Invest. 1999;103:1527-1537.

18. Kaelin WG, Krek W, Sellers WR, et al. Expression cloning of a cDNA encoding a retinoblastoma-binding protein with E2F-like properties. Cell. 1992;70:351-364.

19. Peters LL, John KM, Lu FM, et al. *Ank3* (epithelial ankyrin), a widely distributed new member of the ankyrin gene family and the major ankyrin in kidney, is expressed in alternatively spliced forms, including forms that lack the repeat domain. J Cell Biol. 1995;130:313-330.

20. Laemmli UK. Cleavage of structural proteins during the assembly of the head of bacteriophage T4. Nature. 1970;227:680-685.

21. Steck TL. The organization of proteins in the human red cell membrane. J Cell Biol. 1974;62:1-19.

22. Lehnert ME, Lodish HF. Unequal synthesis and differential degradation of α- and β-spectrin during murine erythroid differentiation. J Cell Biol. 1988;107:413-426.

23. Savvides P, Shalev O, John KM, Lux SE. Combined spectrin and ankyrin deficiency is common in autosomal dominant hereditary spherocytosis. Blood. 1993;82:2953-2960.

24. Jöns T, Drenckhahn D. Identification of the binding interface involved in linkage of the cytoskeletal protein 4.1 to the erythrocyte anion exchanger. EMBO J. 1992;11:2863-2867.

25. Gwynn B, Korsgren C, Ciciotte S, Cohen CM, Peters LL. The gene encoding protein 4.2 is distinct from the mouse platelet storage pool deficiency mutation *pallid*. Genomics. 1997;42:532-535.

26. Alper SL, Natale J, Gluck S, Lodish HF, Brown D. Subtypes of intercalated cells in rat kidney collecting duct defined by antibodies against erythroid band 3 and renal vacuolar H+-ATPase. Proc Natl Acad Sci U S A. 1989;86:5429-5433.

27. Thomas HA, Machen TE, Smolka A, Baron R, Kopito RR. Identification of a 185-kDa band 3-related polypeptide in oxyntic cells. Am J Physiol. 1989;257:C537-C544.

28. Winkelmann JC, Costa FF, Linzie BL, Forget BG. β-spectrin in human skeletal muscle: tissue-specific processing of 3′ β-spectrin pre-mRNA generates a beta spectrin isoform with a unique carboxyl terminus. J Biol Chem. 1992;265:20449-20454.

29. Peters LL, Turtzo LC, Birkenmeier CS, Barker JE. Distinct fetal *Ank-1* and *Ank-2* related proteins and mRNAs in normal and *nb/nb* mice. Blood. 1993;81:2144-2149.

30. Cordell HJ, Todd JA, Lathrop GM. Mapping multiple linked quantitative trait loci in non-obese diabetic mice using a stepwise regression strategy. Genet Res. 1998;71:51-64.

31. Sen S, Churchill GA. A statistical framework for quantitative trait mapping. Genetics. 2001;159:371-387.

32. Churchill GA, Doerge RW. Empirical threshold values for quantitative trait mapping. Genetics. 1994;138:963-971.

33. Southgate CD, Chishti AH, Mitchell B, Yi SJ, Palek J. Targeted disruption of the murine erythroid band 3 gene results in spherocytosis and severe haemolytic anaemia despite a normal membrane skeleton. Nat Genet. 1996;14:227-230.

34. Peters LL, Shivdasani RA, Liu SC, et al. Anion exchanger 1 (band 3) is required to prevent erythrocyte membrane surface loss but not to form the membrane skeleton. Cell. 1996;86:917-927.

35. Brosius FCI, Alper SL, Garcia AM, Lodish HF. The major kidney band 3 transcript predicts an amino terminal truncated band 3 polypeptide. J Biol Chem. 1989;264:7784-7787.

36. Chromosome Committee Data (2003 edition). Encyclopedia of the Mouse Genome, Mouse Genome Informatics Project. Bar Harbor, ME: The Jackson Laboratory. Available at: http://www.informatics.jax.org. Accessed in July 2003.

37. Kennedy SP, Warren SL, Forget BG. Ankyrin binds to the 15th repetitive unit of erythroid and nonerythroid β-spectrin. J Cell Biol. 1991;115:267-277.

38. Lombardo CR, Weed SA, Kennedy SP, Forget BG, Morrow JS. βII-spectrin (fodrin) and βIΣ2-spectrin (muscle) contain NH₂- and COOH-terminal membrane association domains (MAD1 and MAD2). J Biol Chem. 1994;269:29212-29219.

39. Ikeda A, Zheng QY, Rosenstiel P, et al. Genetic modification of hearing in tubby mice: evidence for the existence of a major gene (moth1) which protects tubby mice from hearing loss. Hum Mol Genet. 1999;8:1761-1767.

40. Noben Trauth K, Zheng QY, Johnson KR, Nishina PM. mdfw: a deafness susceptibility locus that interacts with deaf waddler (dfw). Genomics. 1997;44:266-272.

41. Tanner MJA. The structure and function of band 3 (AE1): recent developments. Mol Membr Biol. 1997;14:155-165.

42. Chang SH, Low PS. Regulation of the glycophorin C-protein 4.1 membrane-to-skeleton bridge and evaluation of its contribution to erythrocyte membrane stability. J Biol Chem. 2001;276:22223-22230.

43. De Franceschi L, Olivieri O, Miraglia del Giudice E, et al. Membrane cation and anion transport activities in erythrocytes of hereditary spherocytosis: effects of different membrane protein defects. Am J Hematol. 1997;55:121-128.

44. Joiner C, Franco RS, Jiang M, Franco MS, Barker JE, Lux SE. Increased cation permeability in mutant red blood cells with defective membrane skeletons. Blood. 1995;86:4307-4314.

45. Manno S, Takakuwa Y, Mohandas N. Identification of a functional role for lipid asymmetry in biological membranes: phosphatidylserine-skeletal protein interactions modulate membrane stability. Proc Natl Acad Sci U S A. 2002;99:1943-1948.

46. Diakowski W, Prychidny A, Swistak M, et al. Brain spectrin (Fodrin) interacts with phospholipids as revealed by intrinsic fluorescence quenching and monolayer experiments. Biochem J. 1999;338:83-90.

47. Giorgi M, Cianci CD, Gallagher PG, Morrow JS. Spectrin oligomerization is cooperatively coupled to membrane assembly: a linkage targeted by many hereditary hemolytic anemias? Exp Mol Pathol. 2001;70:215-230.

48. Korstanje R, Paigen B. From QTL to gene: the harvest begins. Nat Genet. 2002;31:235-236.

49. Garner C, Tatu T, Reittie JE, et al. Genetic influences on F cells and other hematologic variables: a twin heritability study. Blood. 2000;95:342-346.

50. Peters LL, Cheever EM, Ellis HR, et al. Large scale, high throughput screening for coagulation and hematologic phenotypes in mice. Physiol Gen. 2002;11:185-193.

51. Platt OS, Brambilla DJ, Rosse WF, et al. Mortality in sickle cell disease: life expectancy and risk factors for early death. N Engl J Med. 1994;330:1639-1644.

52. Platt OS. The acute chest syndrome of sickle cell disease. N Engl J Med. 2000;342:1904-1907.

Identification of quantitative trait loci that modify the severity of hereditary spherocytosis in *wan*, a new mouse model of band-3 deficiency

Luanne L. Peters, Rebecca A. Swearingen, Sabra G. Andersen, Babette Gwynn, Amy J. Lambert, Renhua Li, Samuel E. Lux and Gary A. Churchill